1 and lend additional support to the feasibility of triplet cyclopropylidene to singlet orthogonal allene conversion by spin-orbit interaction. As mentioned in the valence-bond treatment, triplet cyclopropylidene to singlet planar allene is also possible. The molecular-orbital correlations for this are much simpler and are given in Figure 5. It essentially involves the pairing up of the two triplet electrons at the center carbon atom by spin-orbit coupling. We believe this path is less likely because the singlet planar allene has higher energy. The triplet-to-singlet conversion is quite facile in other orthogonal π systems, for example, in the reaction of $O(^3P)$ with singlet carbon suboxide (C_3O_2) to give three singlet carbon monoxides[28] and the reaction of $O(^3P)$ with singlet allene to give singlet ethylene and singlet carbon monoxide.[29] I believe[30] that these arise from the same kind of spin-orbit interaction in perpendicular π systems and should be of interest in the reactions of cumulenes in general. It is suggested that experimentalists and theoreticians may want to look more into such triplet-singlet inversion possibilities. In a recent (1977) simplex-INDO study of energy contours, Dillon and Underwood[10] had allowed that in the region "in which the triplet state is calculated to be more stable than the singlet of the same geometry ... it may reasonably undergo intersystem crossing to the singlet.... We submit that, even if ab initio numerical computations show that the potential surfaces of triplet and singlet cross, a mechanism must still be found to account for the nonvanishing spin-orbit conversion matrix element and for qualitative understanding of the process. In this work we have attempted to find such a mechanism.

Acknowledgment. I thank Drs. Allan Laufer, Morris Krauss, and Wing Tsang for discussions. In particular, Dr. Laufer read the manuscript and gave useful comments. I am especially grateful to Dr. Tsang for encouragment to study organic molecular systems. The hospitality of the colleagues and staff at the NBS Chemical Kinetics Division, headed by Dr. John Herron, is also gratefully acknowledged.

Registry No. Cyclopropylidene, 2143-70-6; allene, 463-49-0.

(28) D. S. Y. Hsu and M. C. Lin, *J. Chem. Phys.*, **68** 4347 (1980); G. Pilz and H. Gg. Wagner, *Z. Phys. Chem.*, **92**, 323 (1974).
(29) P. Herbrechtsmeier and H. Gg. Wagner, *Ber. Bunsenges. Phys. Chem.*, **76**, 517 (1972); J. J. Havel, *J. Am. Chem. Soc.*, **96**, 530 (1974).
(30) Y. N. Chiu and M. S. F. A. Abidi, *J. Phys. Chem.*, **86**, 3288 (1982).

Hydrogen-Evolving Semiconductor Photocathodes. Nature of the Junction and Function of the Platinum Group Metal Catalyst

A. Heller,* E. Aharon-Shalom, W. A. Bonner, and B. Miller

Contribution from Bell Laboratories, Murray Hill, New Jersey 07974. *Received April 23, 1982*

Abstract: Noble metal incorporation in the surface of p-type semiconductor photocathodes to catalyze hydrogen evolution leads to efficient solar to chemical conversion if a set of energetic and kinetic criteria are satisfied: (1) the semiconductor–catalyst junction barrier height must be equal to or greater than that of the semiconductor H^+/H_2 junction; (2) the recombination velocity of photogenerated electrons at the semiconductor–catalyst interface must be low; (3) the overpotential for hydrogen evolution at solar cell current densities ($\sim$30 mA/cm^2) must be minor. Because of substantial differences in the vacuum work functions of Pt, Rh, Ru, and the (redox potential of the) H^+/H_2 couple, the barrier heights for junctions of each of the four systems with p-InP ought to vary widely. Yet experiments show that all p-InP(M)/H^+/H_2 junctions, where M = Pt, Rh, Ru, or no metal, have essentially the same $\sim$0.7-V gain in onset potential for hydrogen evolution relative to Pt/H^+/H_2. We attribute the similarity to the known lowering of metal work functions upon hydrogen alloying. Such alloying increases the barrier height and thereby the gain in onset potential over that anticipated from the vacuum work functions. The barrier height, measured as the limiting value of onset potential gain at high irradiance, approaches in all cases the Fermi level difference of p-InP and H^+/H_2 (0.9 $\pm$ 0.2 eV). That Fermi level pinning by interfacial states is not the cause of the similar barriers is evident from the reversible decrease in onset potential with hydrogen depletion and by a unity diode perfection factor of the p-InP(Rh)/H^+/H_2 photocathode, which indicates no measurable interfacial recombination of photogenerated carriers. In agreement, the quantum efficiency of carrier collection (hydrogen evolution) nears unity. The criterion of low overpotential is met by the expected electrocatalytic effect of the noble metals, manifested in a $\geq 10^4$ increase in fill factor. Introduction of the metal into the semiconductor surface allows a p-InP(Rh)/3 M HCl photocathode to sustain 0.25 A/cm^2 at 0.4 V positive of an identically operating Pt electrode. As expected for a semiconductor/H_2 junction, the onset potential shifts by 62 mV per pH unit, quite close to the theoretical Nernst factor, over the entire pH range. To sustain over the long term the 12% solar power conversion efficiency earlier reported and defined, operation at potentials suitable to produce both hydrogen saturation of the catalyst and the thin surface oxide film (where exposed) is necessary. In cells with strong acids this is met in the region +0.4 to +0.55 V vs. SHE overlapping the maximum solar to hydrogen conversion point, typically at +0.45 V. Thus, with adequately pure solutions, efficiency and stability can be compatible.

Introduction

The generation of fuels or chemicals by coupling photon-induced carrier separation at a semiconductor–liquid junction and an electrolytic reaction into a single integrated system is one of the most interesting prospects for photoelectrochemistry. Many recent publications discuss the chemistry, electrochemistry, and physics of semiconductor photoanodes in which platinum group metals catalyze photoelectrolytic processes.[1-26] Others describe photocathodes on which protons are reduced to hydrogen.[27-36] In this class, p-InP catalyzed by noble metals has proved to have par-

(1) Mollers, F.; Tolle, H. J.; Memming, R. *J. Electrochem. Soc.* **1974**, *121*, 1160.
(2) Bulatov, A. V.; Khidekel, M. L. *Izv. Akad. Nauk SSSR, Ser. Khim.* **1976**, 1902.
(3) Wrighton, M. S.; Wolczanski, P. T.; Ellis, A. B. *J. Solid State Chem.* **1977**, *22*, 17.

0002-7863/82/1504-6942$01.25/0

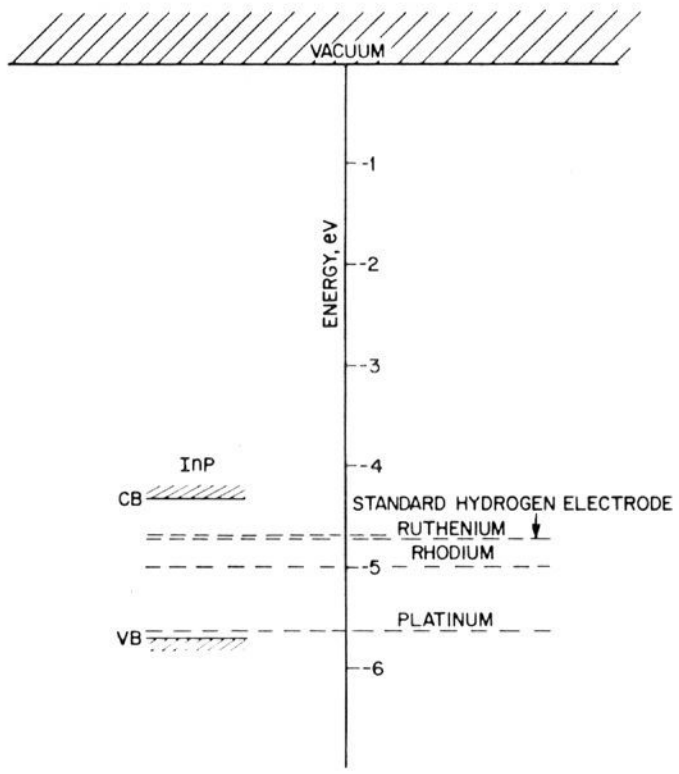

Figure 1. Work functions of Pt, Rh, and Ru, positions of the valence and conduction bands of p-InP, and position of the standard electrode with respect to vacuum.

ticularly favorable properties, and a solar power conversion efficiency of 12% has been achieved.[32-34]

The presence of metals on the semiconductor surface in these photoelectrolytic processes could be expected, from first principles,

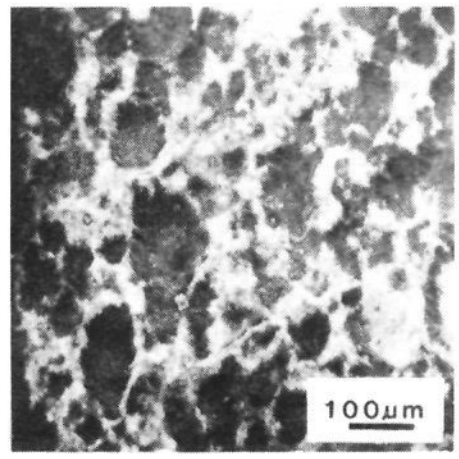

Figure 2. Platinum catalyst islands (light) on p-InP (dark), formed by the photoelectrodeposition–etching–photoelectrodeposition sequence (procedure 1).

to modify the barrier height of the junction considerably. In an ideal Schottky junction between a metal and a semiconductor the barrier height, ψ_B, is the difference between the Fermi level of the semiconductor measured with respect to vacuum (E_F) and the work function of the metal, ϕ_m, corrected for the potential drop across the interfacial dipole layers, Δ_m, equivalent to the Helmholtz layer in solution interfaces.[37-40] Upon illumination of a suitable semiconductor photocathode, the onset potential for hydrogen evolution shifts by an amount ΔV_{oc} with respect to the reversible hydrogen electrode in the same solution. ψ_B is the limit to ΔV_{oc} under high irradiance.

The band positions of InP and of the standard hydrogen electrode (SHE) relative to that of a free electron in vacuo are well-known, as are the vacuum values of work functions[41-49] of the catalyst metals of concern (Figure 1). Accordingly Pt should form an ohmic contact ($\psi_B = 0$) with p-InP; Rh, Ru, and a solution with the potential of the standard hydrogen electrode (SHE) should form junctions with ψ_B up to 0.5, 0.9, and 0.9 eV, respectively. Recent work has, however, shown that, upon dissolution of hydrogen im metals, their work function is reduced.[50-66] In

(4) Kraeutler, B.; Bard, A. J. *J. Am. Chem. Soc.* **1978**, *100*, 5985.
(5) Reiche, H.; Bard, A. J. *J. Am. Chem. Soc.* **1979**, *101*, 3127.
(6) Miller, D. S.; Bard, A. J.; McLendon, G.; Ferguson, J. *J. Am. Chem. Soc.* **1981**, *103*, 5336.
(7) Guruswamy, V.; Keillor, P.; Campbell, G. L.; Bockris, J. O'M. *Sol. Energy Mater.* **1980**, *4*, 11.
(8) Izumi, I.; Dunn, W. W.; Wilbourn, K. O.; Fan, F. R. F.; Bard, A. J. *J. Phys. Chem.* **1980**, *84*, 3207.
(9) Kawai, T.; Sakata, T. *Chem. Phys. Lett.* **1980**, *72*, 87.
(10) Kogo, K.; Yoneyama, H.; Tamura, H. *J. Phys. Chem.* **1980**, *84*, 1705.
(11) Sato, S.; White, J. M. *J. Am. Chem. Soc.* **1980**, *102*, 7206.
(12) Wagner, F. T.; Somorjai, G. A. *J. Am. Chem. Soc.* **1980**, *102*, 5494.
(13) Apple, T. M.; Gajardo, P.; Dybowski, C. *J. Catal.* **1981**, *68*, 103.
(14) Borgarello, E.; Kiwi, J.; Pelizetti, E.; Visca, M.; Graetzel, M. *J. Am. Chem. Soc.* **1981**, *103*, 6324.
(15) Cunningham, J.; Tobin, J. P.; Meriaudeau, P. *Surf. Sci.* **1981**, *108*, L465.
(16) Darwent, J. R. *J. Chem. Soc., Faraday Trans. 2* **1981**, *77*, 1703.
(17) Duonghong, D.; Borgarello, E.; Graetzel, M. *J. Am. Chem. Soc.* **1981**, *103*, 4685.
(18) Giordano, N.; Antonucci, V.; Cavallaro, S.; Lembo, R.; Bart, J. C. *Adv. Hydrogen Energy* **1981**, *2*, 621.
(19) Kalyanasundaram, K.; Borgarello, E.; Graetzel, M. *Helv. Chim. Acta* **1981**, *64*, 362.
(20) Lehn, J. M.; Sauvage, J. P.; Ziessel, R. *Nouv. J. Chim.* **1981**, *4*, 623.
(21) Lehn, J. M.; Sauvage, J. P.; Ziessel, R. *Nouv. J. Chim.* **1981**, *5*, 291.
(22) Sakata, T.; Kawai, T. *Nouv. J. Chim.* **1981**, *5*, 279.
(23) Sakata, T.; Kawai, T. *Chem. Phys. Lett.* **1981**, *80*, 341.
(24) Vidyarthi, S. K.; Bharucha, N. R. *J. Electrochem. Soc.* **1981**, *128*, 2046.
(25) Yoneyama, H.; Nishimura, N.; Tamura, H. *J. Phys. Chem.* **1981**, *85*, 268.
(26) Yoneyama, H.; Shiotani, H.; Nishimura, N.; Tamura, H. *Chem. Lett.* **1981**, 157.
(27) Nakato, Y.; Tonomura, S.; Tsubomura, H. *Ber. Bunsenges. Phys. Chem.* **1976**, *80*, 1289.
(28) Bockris, J. O'M.; Uosaki, K. *J. Electrochem. Soc.* **1977**, *124* 1348.
(29) Jarrett, H. S.; Sleight, A. W.; Kung, H. H.; Gillson, J. L. *Surf. Sci.* **1980**, *101*, 205.
(30) Kautek, W.; Gobrecht, J.; Gerischer, H. *Ber. Bunsenges. Phys. Chem.* **1980**, *84*, 1034.
(31) Dare-Edwards, M. P.; Hamnett, A.; Goodenough, J. B. *J. Electroanal. Chem. Interfacial Electrochem.* **1981**, *119*, 109.
(32) Heller, A.; Vadimsky, R. G. *Phys. Rev. Lett.* **1981**, *46*, 1153.
(33) Heller, A. *Acc. Chem. Res.* **1981**, *14*, 154.
(34) Heller, A.; Vadimsky, R. G.; Johnston, W. D., Jr.; Strege, K. E.; Leamy, H. J.; Miller, B. "Proceedings of the 15th IEEE Photovoltaic Specialists Conference, IEEE, New York 1981", pp 1422–7.
(35) Mettee, H.; Otvos, J. W.; Calvin, M. *Solar Energy Mater.* **1981**, *4*, 443.
(36) Yoneyama, H.; Ohkubo, Y.; Tamura, H. *Bull. Chem. Soc. Jpn.* **1981**, *54*, 404.
(37) Schottky, W. *Phys. Z.* **1940**, *41*, 570.
(38) Bardeen, J. *Phys. Rev.* **1947**, *71*, 717.
(39) Heine, V. *Phys. Rev. A* **1965**, *138*, 1689.
(40) Schluter, M. In "Thin Films and Interfaces"; Ho, P. S., Tu, K. N. Eds.; North-Holland Publishing Co.: New York, 1982.
(41) Harrison, W. A. *J. Vac. Sci. Technol.* **1977**, *14*, 1016.
(42) Eastman, D. E. *Phys. Rev. B* **1970**, *2*, 1.
(43) Herring, C.; Nichols, M. H. *Rev. Mod. Phys.* **1949**, *21*, 185.
(44) Suhrmann, R.; Wedler, G. *Z. Angew. Phys.* **1962**, *14*, 70.
(45) Bouwman, R.; Sachtler, W. M. H. *Surf. Sci.* **1971**, *24*, 140.
(46) Psarouthakis, J.; Huntington, D. R. *Surf. Sci.* **1967**, *7*, 279.
(47) Savitskii, E. M.; Litvak, L. N.; Burov, I. V.; Polyakova, V. P.; Shnyrev, G. D. *Sov. Phys.—Dokl. (Engl. Transl.)* **1970**, *15*, 602.
(48) Balyaeva, M. E.; Larin, L. A.; Kalish, T. V. *Elektrokhimiya* **1976**, *12*, 567.
(49) Gomer, R.; Tryson, G. *J. Chem. Phys.* **1977**, *66*, 4413.
(50) Lundstrom, I.; Shivaraman, M. S.; Svensson, C. *J. Appl. Phys.* **1975**, *46*, 3876.
(51) Lundstrom, I.; Shivaraman, M. S.; Svensson, C.; Lundkvist, L. *Appl. Phys. Lett.* **1975**, *26*, 55.
(52) Lundstrom, I.; Shivaraman, M. S.; Stiblert, L.; Svensson, C. *Rev. Sci. Instrum.* **1976**, *47*, 738.
(53) Shivaraman, M. S.; Lundstrom, I.; Svensson, C.; Hammarshen, H. *Electron. Lett.* **1976**, *12*, 483.
(54) Steele, M. C.; MacIver, B. A. *Appl. Phys. Lett.* **1976**, *28*, 678.
(55) Chauvet, F.; Caratge, P. *C. R. Hebd. Seances Acad. Sci., Ser. B* **1977**, *285*, 153.
(56) Lundstrom, I.; Shivaraman, M. S.; Svensson, C. *Vacuum* **1977**, *27*, 245.
(57) Ruths, J. M.; Fonash, S. J.; Sullivan, T. E. *Ext. Abs., Meeting—Electrochem. Soc., 154th* **1978**, *78-2*, 648.
(58) Ito, K. *Surf. Sci.* **1979**, *86*, 345.
(59) Kawai, T.; Sakata, T. *Chem. Phys. Lett.* **1980**, *72*, 87.

the case of porous metal films on electrodes where two parallel junctions can be formed to the semiconductor, the barrier will tend toward the lower of the semiconductor–metal and semiconductor–electrolyte barriers and will depend upon the microscopic structure and the resistance of the parallel elements.

The purpose of this communication is to interpret, in the perspective of this background, the function of catalysts on the hydrogen-evolving photoelectrodes.

Experimental Section

Preparation of Photocathodes. A p-InP crystal (2×10^{17} cm^{-3} Zn atoms) of about ($8 \times 5 \times 3$) cm^3 was grown by the liquid-encapsulated Czochralski technique[67] and sliced to produce (100) wafers. Final polishing was done on a rotating cloth wetted with 1% bromine in methanol to avoid formation of high surface defect densities. Ohmic contacts were made by evaporating 2000 Å of Au–2% Zn on one of the faces and heating the wafers to 450 °C for 30 s. The wafers were cleaved to 6–10-mm long by 3–6-mm wide pieces. Back copper wire contact leads were attached with silver epoxy and the samples were mounted in an epoxy, sometimes with additional protection from an overcoat of GE Silicone.

Photocathodes with continuous evaporated layers of noble metal catalysts were prepared as follows. The crystals were etched for 10 s with concentrated HCl, allowed to build a thin surface oxide layer by standing 16 h in humid air, and then coated, using E-gun evaporation, with either 200 Å of Pt, 80 Å of Rh, or 100 Å of Ru. Thicknesses accurate to within +50, −10 Å were measured by the Tallysurf technique.

For solution deposition of catalysts on p-InP, two techniques were employed. The first yields islands of the metal over the surface and the second a nearly uniform surface with a few pores visible at 20000×.

Procedure 1. Plating electrolytes were 10^{-3} M solutions of $RuCl_3 \cdot 3H_2O$, K_2PtCl_6 or $Pt(NH_3)_2(NO_2)_2$, and $RhCl_3$ or $Rh_2(SO_4)_3$ in 2–4 M HCl or 4 M $HClO_4$, as appropriate. The mounted p-InP electrodes were etched for 10 s in concentrated HCl, rinsed, and then used as photocathodes in one of the above solutions under 150-W tungsten–halogen illumination against a IrO_2–$Ir(TaO_3)_4$ on Ti or a carbon anode. The photocathode potential was first cycled between −0.1 and +0.2 V vs. SCE at a rate of 5 V/min for 30 s. In the course of such photodeposition of the catalyst, the current density at the SCE potential typically increased by a factor of $\sim 10^4$ (from <10 $\mu A/cm^2$ to 50 mA/cm^2). Next the electrode was cycled between 0 and +0.4 V vs. SCE until a repeating value of current density at the SCE was reached. The electrode was then etched in concentrated HCl until rapid gas evolution indicated substantial damage to the Pt, Rh, or Ru film. Finally, more catalyst was plated under illumination by cycling between +0.1 and +0.5 V vs. SCE. The current density at +0.2 V vs. SCE first increases with the amount of catalyst and then decreases correspondingly after sufficient catalyst has been deposited to absorb ~5% of the light. Were the catalyst films uniform, 5–10 Å would cause 5–10% light absorption.[68-70] Scanning electron microscopy with energy dispersive X-ray analytical capability reveals that the photodeposition–etching–photodeposition process actually produced nonuniform islands and ridges of the catalyst, possibly because the residual catalyst on the etched surface forms sites for nucleation of the metals in the second deposition step. Figure 2 shows a scanning electron micrograph of p-InP surface platinized in this manner.

Procedure 2. This procedure varies from the first essentially by avoiding roughening the surface initially and eliminating the gas-evolving etching of the photodeposited metal. p-InP was washed with methylene chloride, methanol, and water, and cycled 2–3 times in 4 M $HClO_4$ between 0 and −0.7 V vs. SCE under illumination. The requisite amount of metal salt for a 10^{-3} M solution was then added and plating carried out with further cycling or by holding the potential a few millivolts negative of V_{oc}. After the limiting current, checked periodically, declined to about $^1/_2$ of the maximum value achieved because of the growing thickness of the metal film, the resulting electrode shows very few pores at 20000×. Such electrodes have virtual shorts between probes placed on the dry metal film surface 2–3 mm apart.

Table I. ΔV_{oc} Values for p-InP Photocathodes with and without Catalysts

catalyst	catalyst form	solution	ΔV_{oc}	catalyst work function: vacuum	catalyst work function: electrochemical[b]
none, untreated		3 M HCl	0.46		
none, etched		3 M HCl	0.49		
etched, 0.1 M $AgNO_3$ dipped		3 M HCl	0.59		
Pt	islands[a]	3 M HCl	0.65	5.65	5.03
Rh	islands[a]	3 M HCl	0.67	4.98	4.99
Ru	islands[a]	2 M HCl + 100 g of KCl	0.62	4.71	4.80
Pt	evaporated film	4 M HCl	0.57	5.65	5.03
Rh	evaporated film	4 M HCl	0.48	4.98	4.99
Ru	evaporated film	4 M HCl	0.59	4.71	4.80

[a] Procedure 1 in text. [b] From Trasatti (ref 75).

Chemicals. Because the catalysts are sensitive to poisons, purity of the chemicals is critical, particularly for long-term stability. Ultrapure 70% $HClO_4$, concentrated HBr from Alpha Chemicals, and "Ultrex"-grade concentrated HCl from J. T. Baker were used. Reagent-grade materials could be used with freshly prepared samples or in experiments of shorter duration without effect.

Anodes. IrO_2–$Ir(TaO_3)_4$-coated Ti anodes[71,72] were used, but, when experiments required the exclusion of catalyst, carbon anodes were substituted.

Cells. For experiments in which H_2 and O_2 were generated, both electrodes could be placed in one compartment and the gases swept by N_2. Single-compartment cells under N_2 flush were also used in experiments where the charge passed corresponded to accumulating $<10^{-3}$ M halogen. Otherwise, experiments were run in two-compartment cells with 25-cm^2 NAFION membrane or 1-cm^2 fine frit separators. Since mercury from calomel electrodes poisons the catalysts, Ag/AgCl/saturated KCl reference electrodes behind cracked glass separators were used in extended experiments and periodically checked against SCE.

Light Sources. The usual light source was a 100-W tungsten–halogen lamp operated at 7 A to produce a light-limited current density of 50–75 mA/cm^2 in p-InP, 2–3 times that in AM1 solar experiments.[32] An argon ion laser (Spectra Physics Model 172) was employed for varying irradiance experiments. The light flux incident on the cell was measured with a thermopile.

Electrochemical Measurements. Current–voltage behavior was monitored with either a combination of PAR 175 programmer/173 potentiostat–galvanostat or a Pine RDE3 potentiostat/galvanostat. For variation of a second parameter such as pH or light intensity, ΔV_{oc} was measured potentiometrically. To obtain ΔV_{oc}, the i–V curves were measured and the zero-current intercept values of the Pt potential were subtracted from the respective catalyzed or uncatalyzed p-InP electrode values.

Results

The gain in onset for hydrogen evolution, ΔV_{oc}, relative to Pt is shown in Table I for various HCl solutions and a collection of photocathodes. Represented here are bare p-InP as polished, as etched, and as etched and predipped in silver ion, along with the

(60) Li, W. B.; Yoneyama, H.; Tamura, H. *Denki Kagaku oyobi Kogyo Butsuri Kagaku* **1980**, *48*, 570; *Chem. Abstr.* **1981**, *94*, 95157.
(61) Yamamoto, N.; Tonomura, S.; Matsuoka, T.; Tsubomura, H. *Surf. Sci.* **1980**, *92*, 400.
(62) Armgarth, M.; Nylander, C. *Appl. Phys. Lett.* **1981**, *39*, 91.
(63) Poteat, T. L.; Lalevic, B. *IEEE Trans. Electron Devices* **1982**, *ED-29*, 123.
(64) Ruths, P. F.; Ashok, S.; Fonash, S. J.; Ruths, J. M. *IEEE Trans. Electron Devices* **1981**, *ED-28*, 1003.
(65) Yamamoto, N.; Tonomura, S.; Tsubomura, H. *J. Appl. Phys.* **1981**, *52*, 5705.
(66) Fonash, S. J. *J. Appl. Phys.* **1976**, *47*, 3597.
(67) Bonner, W. A. *J. Cryst. Growth* **1981**, *54*, 21.
(68) Coulter, J. K.; Haas, G.; Ramsey, J. B., Jr. *J. Opt. Soc. Am.* **1973**, *63*, 1149.
(69) Kirilova, M. M.; Nomerovannaya, L. V.; Noskov, M. M.; Gorina, N. B.; Polyakova, V. P.; Savitskii, E. M. *Sov. Phys.—Solid State (Engl. Transl.)* **1978**, *20*, 994.
(70) Hass, G.; Hadley, L. In "American Institute of Physics Handbook"; Gray, D. E., Ed.; McGraw-Hill: New York, 1972; p 6-144–6.
(71) Beer, H. B. Netherland Patent Application 6606302; *Chem. Abstr.* **1967**, *67*, 17379.
(72) Smith, G. C.; Okinaka, Y. *Ext. Abstr. Meeting—Electrochem. Soc., 158th* **1980**, *80-2*, Abstract 374.

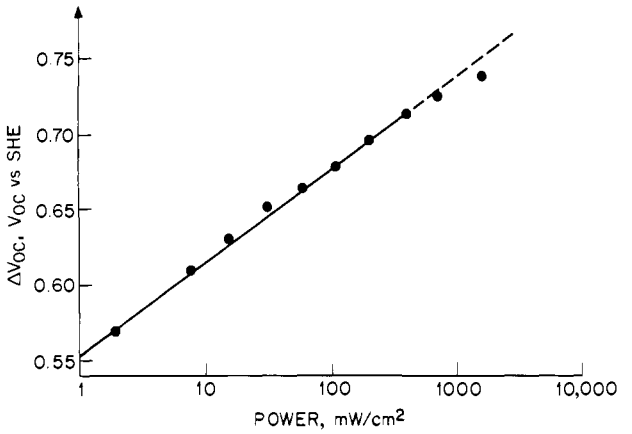

Figure 3. Variation of ΔV_{oc} of the p-InP (Rh) photocathode with irradiance. The light source is an argon ion laser.

noble metal treated surfaces. The silver treatment was earlier shown[34] to improve the i–V characteristics of p-InP photocathodes in the regenerative cell based on the V^{3+}/V^{2+} couple in HCl, importantly without appreciably affecting the poor hydrogen evolution kinetics of this surface. Examples of each of the three noble metal catalyzed photocathodes, p-InP(Pt), p-InP(Rh), and p-InP(Ru), are shown in the two forms, "island" surfaces produced by procedure 1 in the Experimental Section and the evaporated, continuous films of the thicknesses indicated. The latter method yields no visible pinholes at 22 000× on quartz specimens run in parallel.

ΔV_{oc} values in Table I are not corrected for the light loss due to absorption and reflection by the metal films. Such corrections could not alter the relative magnitudes of ΔV_{oc} by more than 30 mV.

From the data in the Table I it is evident that, within the spread of 0.2 V, the values of ΔV_{oc} are quite similar for all these surfaces, whether catalyzed or not, whether homogeneously or irregularly covered by the metals.

The dependence of ΔV_{oc} on irradiance of a p-InP(Rh) island photocathode in 3 M HCl is shown in Figure 3. ΔV_{oc} increases linearly with the logarithm of the irradiance over at least two decades (0.1–1 W/cm²). The slope is in good agreement with 2.303 kT/q; i.e., a 10-fold increase in irradiance increases ΔV_{oc} by 59 mV at 298 K. At 0.1 W/cm² and above, approach of the flat band potential slows the increase. From the highest ΔV_{oc} achieved, it is evident that the flat band potential in 3 M HCl is more positive than 0.75 V vs. SHE and that the barrier height ψ_B, is ≥0.75 eV.

As seen in Figure 4 the p-InP(Rh) photocathode has a 62 mV/pH shift vs. a fixed reference (SCE). The potential of a hydrogen (H_2/H^+) electrode is also shown in Figure 4 for theoretical Nernst behavior. Thus, within experimental error, the catalyzed photocathode parallels the Nernst equation dependence of a H^+/H_2 electrode on pH. The gain in onset potential, ΔV_{oc}, is independent of pH.

Extended cycling of the p-InP(Rh) photocathode in 4 M $HClO_4$ between 0.22 V vs. SHE and V_{oc} results in the i–V characteristics represented by curve I in Figure 5. The power output is improved after the net anodic current excursion associated with momentarily blocking the light when the electrode is at V_{oc} (point A). V_{oc} now increases to point B and the i–V trace becomes immediately that of curve II. However, if the electrode is held for a prolonged time at point B, V_{oc} gradually declines to point C and the first i–V scan thereafter is that represented by curve III. Maintenance of the electrode at any point on curve III more negative in potential than point C restores the characteristics to those of curve II.

A stable operating domain DE exists on curve II near the maximum power conversion region where passage of 3600 C/cm² (20-h operation at 50 mA/cm²) causes only a 30% decline, restored on bringing the electrode to point B.

Catalysis by photoelectrodeposited Pt islands is very graphically demonstrated in the log plot of the i–V characteristics of the

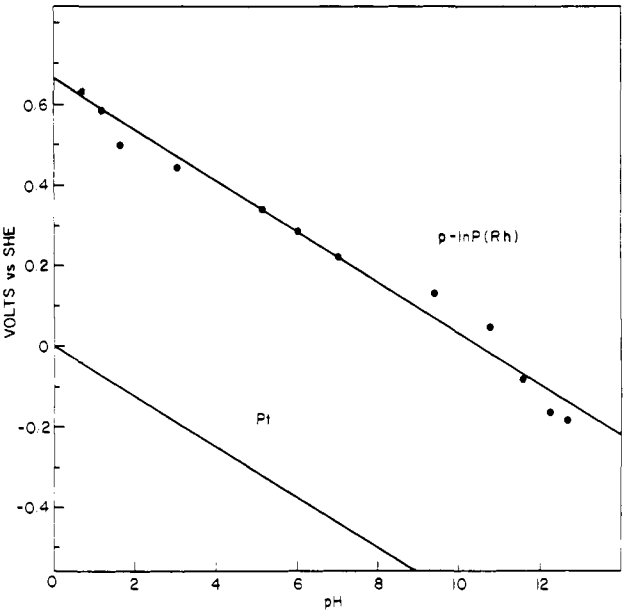

Figure 4. Dependence of V_{oc} on pH for p-InP (Rh). The electrolyte was initially 0.25 M HCl–0.25 M H_3PO_4 and the pH was increased by increments of 5 M NaOH solution. The solid line is the theoretical curve for the hydrogen electrode at solid Pt.

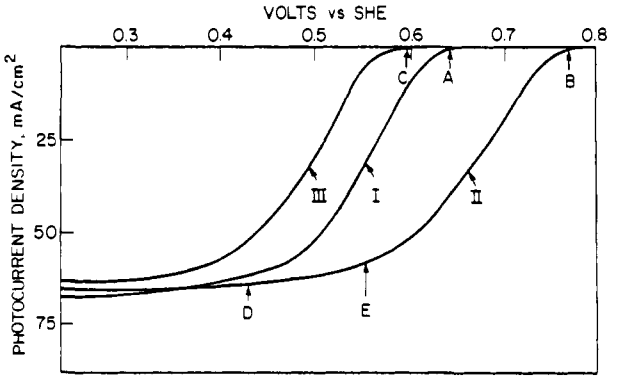

Figure 5. Curve I results after extended cycling of a p-InP(Rh) photocathode in 4 M $HClO_4$ between 0.22 V vs. SHE and V_{oc}. If the light is blocked when the electrode is at V_{oc} (A), reapplication of light gives a V_{oc} increase to B and the immediate i–V characteristic in curve II. Prolonged standing at B results in V_{oc} decline to C with the first i–V scan thereafter being given by curve III. Any potential held negative of C restores activity to that of curve III. A stable operating domain DE exists on curve II near its maximum conversion efficiency point. Here 3600 C/cm² (24-h operation) causes only a 30% decline, restored by the above attainment of B (scan rate 10 V/min).

photocathode in 4 M $HClO_4$ shown in Figure 6. At 0.45 V vs. SHE a 10^4-fold increase in photocurrent is observed. A lesser factor is found as the SHE potential is approached, but it should be noted that the steady-state currents at a Pt electrode anywhere on this plot would be too low to be on scale.

The results of experiments on p-InP(Rh) photocathodes in 3 M HCl under high irradiance are presented in Figures 7 and 8. The former shows that, at sufficiently high levels of irradiance, current densities of >0.25 A/cm² are maintained at +0.25 V vs. SHE. This current density is attained at Pt only near −0.25 V vs. SHE. Thus, ΔV at this current density is 0.5 V.

In Figure 8 the straight line represents the theoretical current efficiency for the p-InP(Rh) photocathode at the fixed +0.25 V vs. SHE potential, calculated with the assumption that every photon incident from the argon ion laser onto the cell window is converted to an electron–hole pair and every carrier is collected. The ratio of the measured and calculated photocurrents at a given irradiance is the quantum efficiency. One sees the quantum efficiency is high (>80%) and fairly constant to photocurrents near 0.1 A/cm². This drops to ~40% at 0.25 A/cm². A sub-

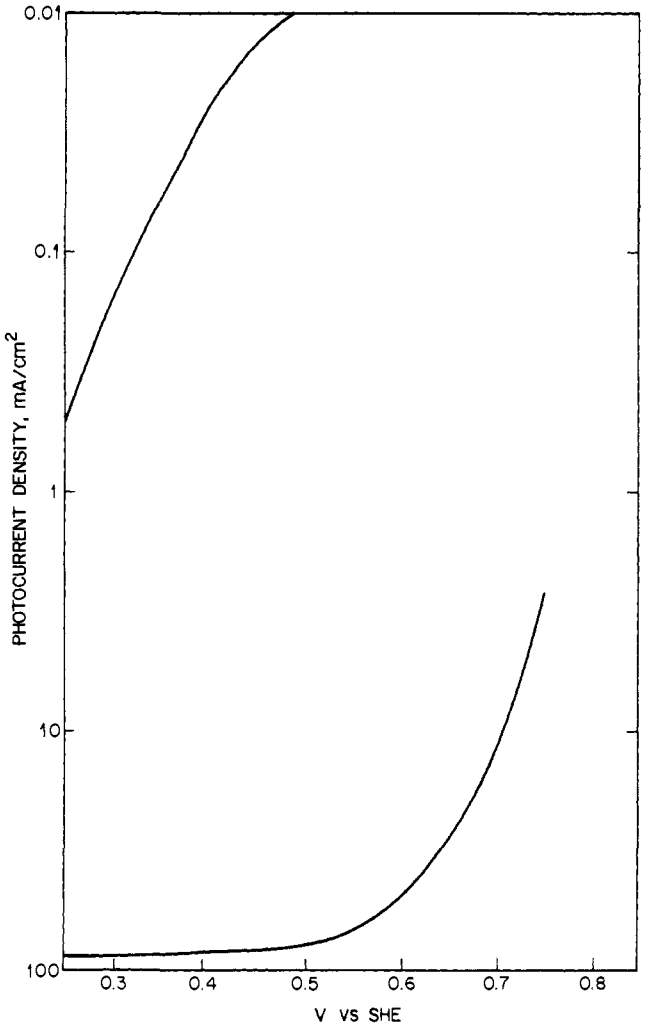

Figure 6. Effect of incorporation of Pt catalyst islands in the surface of p-InP on the current–voltage characteristics of the photocathodes in 3 M HCl. Upper curve (lower current) is that of an uncatalyzed electrode, the lower that after Pt deposition (scan rate 10 V/min).

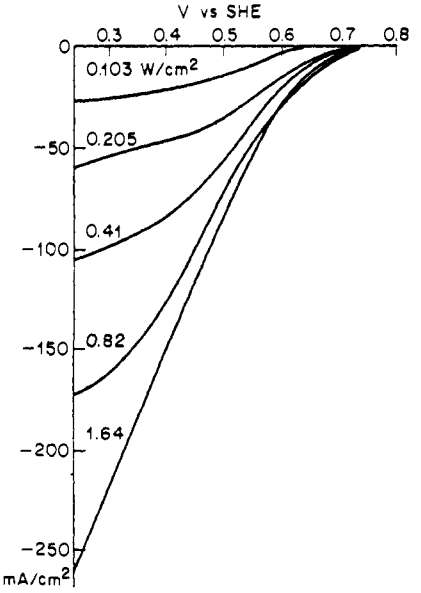

Figure 7. Current–voltage characteristics of the p-InP (Rh) photocathode in 3 M HCl at the varying levels of irradiance (argon ion laser) indicated on the traces.

stantial portion of this drop is due to resistance losses shifting the potential to more positive values.

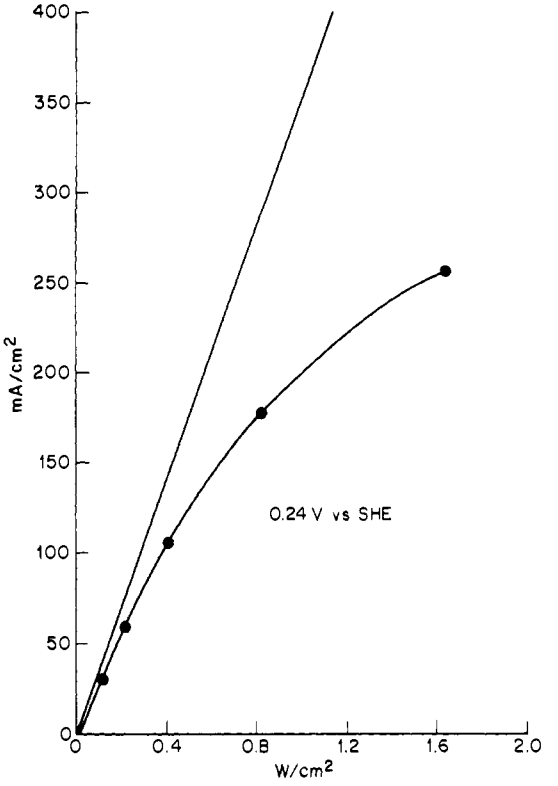

Figure 8. Dependence of the current efficiency of the p-InP (Rh) photocathode (in 3 M HCl, at +0.24 V vs. SHE) on irradiance (argon ion laser). The straight line represents the theoretical limit to the photocurrent, unit quantum efficiency.

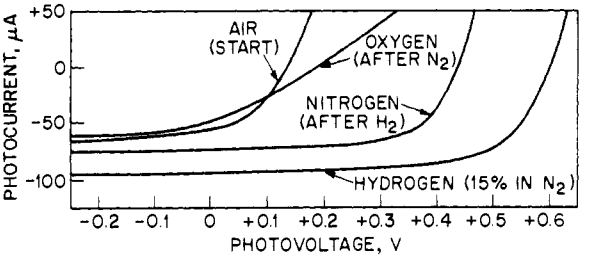

Figure 9. Current–voltage curves for a dry Schottky junction photovoltaic cell (uniform Rh plated by procedure 2 on p-InP). The sequence of gaseous environments is (1) air, (2) 15% H_2, (3) 40-min flush of N_2, and (4) oxygen (scan rate 100 mV/s).

In an earlier paper we indicated that the p-InP(Ru) photocathode in 4 M HCl requires allowing it to reach V_{oc} once every 20 min to regenerate maximum efficiency.[32] With high-purity 4 M $HClO_4$ the p-InP(Ru) photocathode at +0.45 V vs. SHE shows considerably improved stability, the current density decreasing from 60 to 40 mA/cm² over a 20-h period. Again, the current density is restored to its original value by a 30-s hold at +0.74 V vs. SHE in the absence of illumination. The charge density passed in such a 20-h experiment is 3600 C/cm². The loss in limiting photocurrent density for this island surface due to metal layer coverage corresponds to only a 7 ± 3 Å film, from the known optical constants of uniform surfaces. From the thickness of the metal film, from its density of 12 g/cm², and from the equivalence of 3600 C/cm² to 0.037 g-atom of hydrogen evolved, we calculate the catalyst turnover number to $^2/_3$ of the original efficiency to be 10^7.

In order to examine the work function shifts attributable to various atmospheres (H_2, N_2, air, or O_2), independently of the photoelectrochemical process, we obtained current–voltage curves for various dry noble metal–p-InP diodes using a low force probe to the metal film. These were prepared by procedure 2 in the Experimental Section to achieve nearly homogeneous coatings. The curves for Rh on p-InP are typical of the various metals and

are shown in Figure 9. It is clear that the barrier is increased by hydrogen absorption, reduced by nitrogen scrubbing, and made very small by exposure to air or oxygen.

Discussion

Nature of the Semiconductor–Catalyst Junction. The maximum gain in onset potential for hydrogen evolution with respect to a reversible Pt cathode is limited to the barrier height at the junction. When a metallic phase covers the entire semiconductor surface without alloying or chemically reacting, and when nonstoichiometric compositions and carrier recombination in interfacial states are absent

$$\psi_B = E_f - \phi_m + \Delta_m \quad (1)$$

where Δ_m is the potential drop across the interfacial dipole layer.

In the absence of a catalyst layer, the upper limit of ψ_B at hydrogen evolution is

$$\psi_B = E_F - \phi_H + \Delta_H \quad (2)$$

where ϕ_H is the work function of hydrogen absorbed on the semiconductor surface and Δ_H is the potential drop across the Helmholtz layer.[73,74] Because of the analogy between eq 1 and 2, we shall refer to ϕ_m as "metallic" hydrogen. When the catalyst is nonhomogeneously dispersed on the surface of the semiconductor, forming islands that are spaced within distances comparable to or shorter than the minority carrier diffusion length, there are two parallel junctions. The ideal barrier height is now the lower of the two that can be formed, since no potential exceeding the height of the lower barrier can be sustained.

The vacuum work functions of the catalysts Pt, Rh, and Ru vary over a 0.9–V span, as noted earlier. Trasatti[75] has presented values of "electrochemical work functions" applying to a catalyst–aqueous acid interface. These contain the influence of the surface dipole effect of water as well as possible products of water and the catalyst surface and are calculated in part through correlation to potentials of zero charge. These calculations particularly shift the value of Pt from the vacuum value, reduce the spread of the three metals to 0.25 V, and move the average value to about 0.2 V positive (electrochemical scale) of the hydrogen electrode. The procedures attempt to avoid the influence of adsorbed hydrogen but the degree of this effect on Trasatti's work function cannot be clearly ascertained from this reference.

If we apply vacuum work function values, the Fermi level of Pt is at the valence band edge in InP, leading to a negligible p-InP/Pt junction barrier height and an expectation of ohmic contact behavior. On the same basis the barrier heights between p-InP, and Rh and Ru, should be 0.5 and 0.9 V, respectively (Figure 1). Our measurements show that in hydrogen-generating photocathodes all three metals produce barriers of equal height. Trasatti's data would give barrier heights between 0.1 and 0.35 V.

For p-InP (catalyst) photocathodes in 4 M $HClO_4$ we have observed ΔV_{oc} values as high as 0.8 V. Thus, a barrier height of $\geq$0.8 V is realizable with all three metals. Indeed, uncatalyzed surfaces appropriately prepared give high ΔV_{oc} (Table I), even though the curves are very flat near open circuit and the potential values are susceptibile to the effects of corrosion and other mixed potential phenomena. Thus, the p-InP/oxideH^+/H_2 barrier is substantially this high also.

We explain the similarity in barrier heights primarily by the decrease in work function upon dissolution of hydrogen in the metals. When hydrogen saturated, all three metals have the work function of "metallic" hydrogen, i.e., hydrogen adsorbed on the semiconductor at saturation pressure. Hydrogen-evolving photocathodes operate, by definition, at the phase separation/saturation point and have the hydrogen thermodynamic value.

The experiments with dry metal–p-InP diodes in various gaseous environments support the contention that hydrogen permeation strongly reduces the work function. The effects of air or oxygen

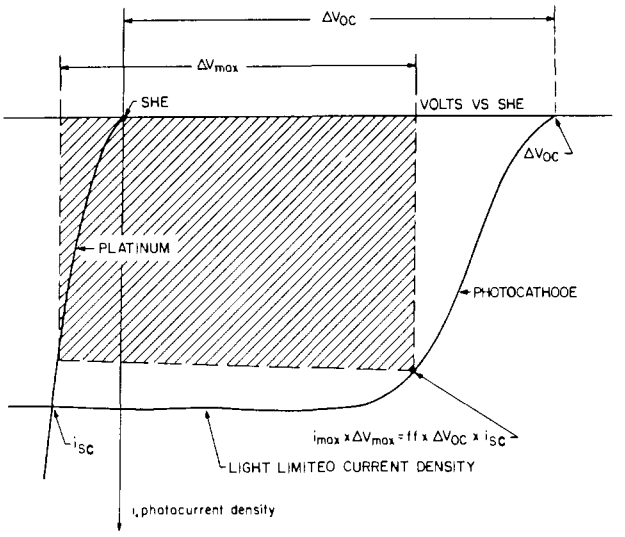

Figure 10. Definition of the fill factor (ff) for a hydrogen-generating photoelectrochemical cell. The onset potential for hydrogen evolution is ΔV_{oc}. The equivalent of the short-circuit current density, i_{sc}, is the current density at the intersection of the platinum and photoelectrode curves. The maximum light to chemical conversion is at $i_{max}\Delta V_{max}$.

introduction on the diode characteristics are strikingly parallel to those of the photoelectrochemical experiments described in Figure 5, where extended positive potential excursions remove hydrogen and drop the barrier height and cathodic operation restores it. While sustained hydrogen evolution is necessary for maintenance of the barrier height, an appropriate oxide film to reduce recombination[76–80] must also be retained. Thus, the hydrogen evolution is stable only over the potential range of 0.4–0.55 V vs. SHE.

Our model explaining the behavior of the semiconductor (photocatalyst) is also consistent with the high-vacuum, low-hydrogen-pressure measurements on the change in work function of Pt upon hydrogen chemisorption[81,82] and is corroborated by recent studies on solid-state hydrogen sensors.[50–66] Both sets of results point to a reversible decrease in the work functions of platinum group metals as they "alloy" with hydrogen.

Ideality of the Junction. The dependence of ΔV_{oc} on incident power I (Figure 3) follows the theoretical relation

$$\Delta V_{oc} = A_0(2.303kT/q) \log (I/I_0 + 1) \quad (3)$$

where q is the electron charge and I_0 is the (unmeasured) dark current. A_0, the diode quality factor, is experimentally found equal to unity (the slope of the ΔV_{oc} vs. log $[(I/I_0) + 1]$ plot is 59 mV). The junction can be considered to be behaving ideally: photogenerated electrons do not recombine at the semiconductor–metal or semiconductor–solution interfaces.

The origin of the ideal response is the simultaneous reduction in surface recombination by the thin tunnelable oxide film, combined with the achievement of the full barrier height, through hydrogen saturation of the photoactive interface.

As seen in from Figure 5, such ideality is not sustained if the surface becomes depleted of hydrogen, or if the oxide film is reduced.

(73) Butler, M. A.; Ginley, D. S. *J. Electrochem. Soc.* **1978**, *125*, 228.
(74) Butler, M. A.; Ginley, D. S. *J. Mater. Sci.* **1980**, *15*, 1.
(75) Trasatti, S. *J. Electroanal. Chem.* **1971**, *33*, 351.
(76) Heller, A. In "Photoeffects at Semiconductor–Electrolyte Interfaces"; Nozik, A., Ed.; American Chemical Society: Washington, DC, 1981; *ACS Symp. Ser.*, No. 146, p 57.
(77) Heller, A.; Miller, B.; Lewerenz, H. J.; Bachmann, K. J. *J. Am. Chem. Soc.* **1980**, *102*, 6555.
(78) Heller, A.; Miller, B.; Thiel, F. A. *Appl. Phys. Lett.* **1981**, *38*, 200.
(79) Heller, A.; Lewerenz, H. J.; Miller, B. *J. Am. Chem. Soc.* **1981**, *103*, 200.
(80) Lewerenz, H. J.; Aspnes, D. E.; Miller, B.; Malm, D. L.; Heller, A. *J. Am. Chem. Soc.* **1982**, *104*, 3325.
(81) Voronina, G. F.; Larin, L. A.; Kalish, T. V. *Elektrokhimiya* **1978**, *14*, 297.
(82) Gorodetskii, V. V.; Nieuwenhuys, B. E.; Sachtler, W. M. H.; Boreskov., G. K. *Surf. Sci.* **1981**, *108*, 225.

Function of the Catalyst. While the catalyst does not change appreciably the barrier height, it is evident from Figure 5 that it increases dramatically the equivalent of the fill factor of solar cells. This equivalent fill factor is defined in Figure 10.

The maximum conversion point for the p-InP(Ru) photocathode in HCl is near +0.45 V vs. SHE. As shown in Figure 6 the catalyst increases the photocurrent density at this point by 10^4. It is relevant to note that the very slow rate of proton reduction in the absence of a catalyst makes possible the operation of the regenerative cells p-InP/VCl_3–HCl/C,[76,77] where the redox potential of the electrolyte is negative of SHE. In the presence of traces of a catalyst, the thermodynamically unstable cell is destroyed, and the electrolyte turns into green V(III) with concomitant hydrogen evolution.

Efficiency at High Current Densities. Photoelectrochemical solar cells are often less efficient when operated under high irradiance because of concentration overpotentials due to mass transport limitations and also solution and kinetic impedances. (Water-oxidizing photoanodes have the advantage that the reactant concentration approaches 55 M and local pH changes can be avoided by concentrated buffers (or acid or base concentration.)

With p-InP (catalyst) photocathodes in acids, moderate concentration of sunlight becomes feasible because of the reduced impedance of the efficient catalysts and the high mobility of protons. Figure 7 shows a photocurrent density of 0.25 A/cm^2 at SCE potential where the quantum efficiency is ~0.4 (Figure 8). More importantly, the operating advantage of about 0.5 V over a Pt cathode is retained. Even at 0.1 A/cm^2, the equivalent of 4-fold concentrated AM1 sunlight output, the quantum efficiency is 0.8, including window reflection and solution absorption.

Conclusions

Hydrogen-evolution catalysts like Pt, Rh, and Ru alloy hydrogen. Hydrogen alloying lowers the work function of the metals and increase the height of barriers formed between the catalysts and p-type semiconductors. Since the barrier height determines the saving in applied potential for hydrogen evolution at the photocathode with respect to that at a reversible (platinum) electrode, hydrogen dissolution improves the photocathode's performance. The work functions of the catalyst metals reach a plateau at hydrogen saturation, making the height of the barriers similar for all hydrogen-alloying metals, even though their initial vacuum work functions may vary considerably. The basis for the similarity is the following: If a hydrogen-alloying metal is in equilibrium with the H_2/H^+ couple, its Fermi level equals the hydrogen electrode's potential. At constant pH this is determined solely by the partial pressure of hydrogen. Thus, at hydrogen saturation (partial pressure = 1 atm) all hydrogen-alloying metals that are saturated with hydrogen have equal Fermi levels (work functions).

In this view, the barrier for the p-semiconductor/H_2(satd)/H^+ junction is not changed by the presence or absence of catalyst at the semiconductor surface, provided there are no interfacial chemical reactions between the metal and the semiconductor and interfacial states for carrier recombination are not introduced. It should, therefore, be feasible to stabilize hydrogen-evolving photocathodes that react with a solvent or with an electrolyte by prior coating of the semiconductor with a catalyst film of good integrity. Barrier heights and the consequent gain in onset potential for hydrogen evolution would not suffer and there would be a gain in fill factor. The metal would however absorb some of the light and cause problems identical with those of current MOS and MIS cells, or related hybrid cells with electrolyte contacts whose losses we have already measured.[83]

(83) Menezes, S.; Heller, A.; Miller, B. *J. Electrochem. Soc.* **1980**, *127*, 1268.

Cases where there are no interfacial reactions between the semiconductor and the catalyst metal and where there are no interfacial sites for carrier recombination are known. InP forms a 4–10-Å thick layer of oxide[80] which performs the dual role of physical barrier to the catalyst metal and surface stabilization, reducing the interfacial recombination rates.[33,76] In another case, the oxide on Si is a barrier to interdiffusion and to silicide formation with Pt.[66] The oxide is also effective in eliminating surface states associated with "dangling", "rearranged", or "weak" chemical bonds that are sites for carrier recombination.[32–34,76–80] The presence of the thin oxide layer on InP is assured by anodization at the onset potential for hydrogen evolution. Application of more positive potentials depletes the hydrogen in the catalyst and lowers the barrier height. Formation of oxide at more negative potentials is slower and less effective.

The above conclusions have important implications for photoelectrolysis with particulate suspensions of catalyst-coated semiconductors, including mixtures of p- and n-type particles or particles having both n- and p-type domains, where external bias is not feasible. When hydrogen is evolved at a site, the catalyst work function is reduced and a barrier favoring further electron transport to the surface is formed with a p-type particle or domain. In the absence of hydrogen, or upon incorporation of oxygen, the work function is increased, and a barrier favoring hole transport to the surface results in an n-type particle or domain. Since saturation of the catalyst with hydrogen is not instantaneous, the rate of hydrogen evolution should be greatly accelerated by the coupled work function decrease and barrier height increase upon dissolution of hydrogen in the catalyst. This interesting phenomenon should be observable as an induction period prior to a steep rise in hydrogen evolution.

Since the junction is in essence a semiconductor/hydrogen junction, its barrier height is sensitive to the partial pressure of hydrogen but does not depend on pH because, unlike hydrogen, protons do not dissolve in the catalyst lattice and thus do not change its Fermi level. While the barrier height and the gain in onset potential for hydrogen evolution are insensitive to pH, the absolute value of the onset potential for hydrogen evolution shifts with pH, because the proton concentration in solution defines the potential at which hydrogen evolution begins. No net gain is achieved with pH variation if the counterelectrode reaction is similarly pH dependent, as is the case for oxygen evolution. Nothing can be gained by varying the pH: The external bias required for electrolysis will always exceed the reversible cell voltage minus the barrier height, a difference actually reached at very high irradiance. At moderate levels of irradiance of ideally performing photocathodes such as these, the gain in onset potential will increase by 59 mV per decade irradiance at 298 K.

The overall effect of the noble metals on p-InP is essentially that of a classical catalyst; the apparent exchange currents of the desired reaction are increased by many orders of magnitude while the open-circuit value, onset potential in this context, is basically not affected. By accelerating the chemical process of hydrogen evolution the catalyst reduces reaction impedance. In the presence of catalysts, the photoelectrolytic reduction of protons is fast enough in strongly acid solutions to support current densities similar to those practiced by today's electrolytic industry, while maintaining a substantial voltage saving over metallic electrodes. Such current densities make feasible, and indeed encourage, the possible economies of concentration of sunlight.

Acknowledgment. The assistance of C. J. Doherty in the deposition of the metal films and in measuring their thickness, of H. Temkin in making electrical contacts, of G. Celler in the argon ion laser experiments, and of D. Colavito in various phases of this work is gratefully acknowledged.

Registry No. InP, 22398-80-7; Pt, 7440-06-4; Rh, 7440-16-6; Ru, 7440-18-8.